Targeting Several Biologically Reported Targets of Glioblastoma Multiforme by Assaying 2D and 3D Cultured Cells

Yudibeth Sixto-López
Instituto Politecnico Nacional Escuela Superior de Medicina
Emilie Marhuenda
Ecole Nationale Superieure de Chimie de Montpellier
Juan Benjamin García-Vazquez
Instituto Politecnico Nacional Escuela Superior de Medicina
Jonathan Fragoso-Vazquez
Instituto Politecnico Nacional Escuela Superior de Medicina
Martha Cecilia Rosales-Hernández
Instituto Politecnico Nacional Escuela Superior de Medicina
Oscar Zacarías-Lara
Instituto Politecnico Nacional Escuela Superior de Medicina
David Méndez-Luna
Instituto Politecnico Nacional Escuela Superior de Medicina
José Antonio Gómez-Vidal
Universidad de Granada
David Cornu
Ecole Nationale Superieure de Chimie de Montpellier
Norbert Bakalara
Ecole Nationale Superieure de Chimie de Montpellier
Jose Correa Correa Basurto (corrjose@gmail.com)
Instituto Politécnico Nacional Escuela Superior de Medicina https://orcid.org/0000-0002-4973-5265

Original Article

Keywords: Glioblastoma multiforme, HDAC, GPER, ER, NOX, 3D cell culture

Posted Date: February 10th, 2021

DOI: https://doi.org/10.21203/rs.3.rs-180994/v1

Version of Record: A version of this preprint was published at Cellular and Molecular Neurobiology on March 19th, 2021. See the published version at https://doi.org/10.1007/s10571-021-01072-9.

Abstract

Glioblastoma multiforme (GBM) is account for 70% of all primary malignancies of the central nervous system. Median The survival of human patients after treatment is around 15 months. There are However, several biological targets which have been reported that can be pursued using ligands with varied structures to treat this disease. In our group, we have developed several ligands that target a wide range of proteins involved in anticancer effects, such as histone deacetylase (HDACs), G protein-coupled estrogen receptor 1 (GPER), estrogen receptor-beta (ERβ), and NADPH oxidase (NOX), that were screened on bidimensional (2D) and tridimensional (3D) GBM stem cells like (GSC). Our results show that some HDAC inhibitors show antiproliferative properties at 21-32 μM as well as . These results suggest that in this 3D culture, HDACs could be the most relevant targets that are modulated to induce the antiproliferative effects that require in the future further experimental studies.

Introduction

Glioblastoma multiforme (GBM) is one of the most common glial tumors, presenting poor prognosis, and less than 5 % survival over the 5 years after initial diagnosis (Liu et al. 2006; Kim et al. 2012; Singh et al. 2004). Multiple therapeutic strategies and biomarkers have risen over years, in this study we selected some of them in order to evaluate potential anti migratory or anti proliferative effect, leading potentially to interesting therapy for GBM during deeper investigations. It has been demonstrated that histone deacetylases (HDACs,),(able to remove acetyl groups from histones protein on DNA) (Was et al. 2019; Lee et al. 2017), displays aberrant expression in cancer. HDACs regulate the expression and activity of numerous proteins involved in cancer initiation, proliferation and progression and seems to be a potential targets against GBM (Yelton and Ray 2018; Lee et al. 2017). Some HDAC inhibitors already developed exhibit hydroxamic acid groups that chelate pivotal Zn^{+2} ions to the catalytic activity of the enzyme (Rajak et al. 2013), but due to a lack of specificity of those compounds, other chemical strategies have been employed to reach the nonpolar cavities of HDACs (Rajak et al. 2013; Wang 2009).

G protein estrogen receptor (GPER) are implicated in diverse biological effects, including regulation of immune, endocrine, neuronal, and cardiovascular functions. In cancer GPER activation is already well described as regulating cell growth and proliferation in several cell line, migration, and apoptotic cell death, but have not been studied in Glioma. Consequently, the use of GPER modulators to explore his role in GBM proliferation and migration appear as a great tool for *in vivo* studies, as well as possible target to treat GBM (Feldman and Limbird 2017). Estrogens have shown implication in development of gliomas, estrogens appear having neuroprotective effects and improves glioblastoma outcome for women (Wan et al. 2018) Lan et al. 2017). Want et al. reported higher expression of ERs receptor in glioma cells in comparison to glial cells (Wan et al. 2018) in which and ERβ appearing as a tumor suppressor in GBM (Liu et al. 2018). Consequently ERβ also appear as a promising target to treat GBM (Lan et al. 2017; Zhou et al. 2019).

Free radicals in GBM play an important role in cell proliferation being the NADPH oxidase (NOX) as putative targets for cancer therapy. NOX family is the main source of reactive oxygen species (ROS) (Meitzler et al. 2014) which could be an important mediator of neuroinflammation Pristimerin Inhibits MMP-9 Expression and Cell Migration Through Attenuating NOX/ROS-Dependent NF-κB Activation in Rat Brain Astrocytes Challenged with LPS (Yang et al. 2020). The use of NOX inhibitors has been reported to inhibit invadopodium formation, the inflammatory response, and cancer cell migration *in vitro*. Furthermore, NOXs as pharmacological targets appear as an interesting strategy for GBM treatment (Munson et al. 2013; Nayernia et al. 2014).

In this study, we explored a diverse set of ligands containing a wide range of functional groups as possible therapeutic agents to treat GBM. Then, 26 compounds were synthetized, including NADPH oxidase inhibitors HDAC inhibitors (**Ia-Ib)**, ER modulators (**IIa-IId, IIIa-IIId**), HDAC inhibitors (**IVa-IVb, VIa-VIg**) and GPER inhibitors (**Va-Vd**). ER modulators, GPER inhibitors, and NADPH oxidase inhibitors. Then, we performed a first preliminary screening in 2D and 3D cell culture to observe potential anti proliferative and/or anti migrating effect on Glioblastoma Stem Cell (GSC). This study is a first step leading to a selection on compound for future and deeper *in vitro* and *in vivo* investigations.

Materials And Methods

Chemical synthesis

All commercial grade reagents were used without further purification. Analytical thin-layer chromatography (TLC) was performed on silica gel 60 F254-coated aluminum sheets (0.25 mm thickness) with a fluorescent indicator. Visualization was accomplished with UV light (254 nm). Flash chromatography was performed using silica gel 60 (230-400 mesh). Melting points were determined in open capillary tubes with an IA 91000 electrothermal melting point apparatus (Electrothermal, Bibby Scientific, Staffordshire, ST15 OSA, UK) and were uncorrected. ^{1}H and ^{13}C NMR spectra were recorded on either Bruker Avance III 750 or 400 MHz spectrometers or on a 500 MHz Varian System using deuterated dimethyl sulfoxide (DMSO-d_6) or chloroform ($CDCl_3$) as the solvent and TMS as the internal standard. Chemical shifts are given in ppm (δ) and are referenced to TMS as the internal standard. Coupling constant values are quoted in Hertz, with normal abbreviations (s, singlet; d, doublet; t, triplet; br, broad; m, multiplet). For complete data assignments, 2D HSQC and HMBC NMR spectra were used. IR spectra were obtained on a Spectrum 2000 Perkin Elmer FT-IR spectrometer. Only significant absorption bands are shown with absorption values expressed as wavenumbers (cm^{-1}). Electrospray ionization (ESI) high-resolution mass spectrometry was performed with a Bruker micrQTOF-Q II instrument and an Agilent 6545 Q-TOF LC/MS. The chemical purity was determined by HPLC using an Agilent 1200 Infinity Series system.

Synthesis of NADPH oxidase inhibitors Ia-Ib

*3,3'-Dimethoxy-5,5'-dipropyl-(1,1'-biphenyl)-2,2'-diol (***Ia***).* The reaction was carried out as previously described by our group (Macias Perez et al. 2017). Heptahydrate ferrous sulfate (0.075 g, 0.3 mmol) and potassium persulfate (0.81 g, 3 mmol) were added to a solution of 2-methoxy-4-propylphenol (1 g, 6 mmol) in 200 mL of hot water/MeOH (3:1 v/v). The mixture was boiled and stirred for 1 h. After cooling to room temperature, the precipitate was collected and dissolved in 100 mL of a 4 N aqueous solution of NaOH. Subsequently, the crude material was precipitated by the addition of 100 mL of a 6 N aqueous solution of HCl. The resulting precipitate was filtered and washed with hot (90 °C) deionized water (3 × 100 mL) and hot methanol (1 × 100 mL). The resulting solid was purified by flash column chromatography with hexane/EtOAc (1:1) to obtain **Ia** in 66 % yield. Full chemical characterization was reported (Macias Perez et al. 2017).

*1,1'-(6,6'-Dihydroxy-5,5'-dimethoxy-(1,1'-biphenyl)-3,3'-diyl)-bis-(ethan-1-one) (***Ib***).* The reaction was carried out as described elsewhere (Macias Perez et al. 2017). Ferrous sulfate heptahydrate (0.075 g, 0.3 mmol) and potassium persulfate (0.81 g, 3 mmol) were added to a solution of apocynin (1 g, 6 mmol) in 200 mL of water (90 °C). The reaction mixture stirred in a boiling water bath for 0.5 h. After cooling to room temperature, the precipitate was collected and dissolved in 100 mL of a 4 N aqueous solution of NaOH. Subsequently, the product was precipitated by adding 100 mL of a 6 N aqueous solution of HCl. The final precipitate was filtered and washed with deionized water at 90 °C (3 × 100 mL) and hot methanol (1 × 100 mL) to obtain **Ib** in 63 % yield. Full chemical characterization was reported (Macias Perez et al. 2017).

Synthesis of acrylonitriles IIa-IId as ERβ modulators

The synthesis of nitriles followed a previously reported method (Vaccaro et al. 1996; Martinez-Archundia et al. 2018). A solution of 40 % aqueous KOH (0.23 mL/mmol nitrile) was diluted with EtOH (0.46 mL/mmol nitrile) and added at room temperature to a solution of arylaldehyde (1.1 equiv) and arylacetonitrile (1.0 equiv) in EtOH (0.35 mL/mmol nitrile). The resulting mixture stirred for 3 h at the same temperature, quenched with water (5 mL) and 5 % aqueous HCl (1.5 mL), extracted with EtOAc (3 × 25 mL), washed with brine, dried over Na_2SO_4, and concentrated in vacuo. The residue was purified by flash chromatography on silica (hexane/EtOAc 9:1) to give acrylonitriles **IIa**-**IId**.

(Z)-2,3-Bis(4-fluorophenyl)acrylonitrile (**IIa**). Application of the typical procedure using 2-(4-fluorophenyl)acetonitrile (0.2 g, 1.48 mmol) and 4-fluorobenzaldehyde (0.2 g, 1.61 mmol) gave acrylonitrile **IIa** (0.35 g, 97 %). The spectral data of **IIa** were identical to those reported (Buu-Hoï et al. 1957).

(Z)-2,3-Bis(4-bromophenyl)acrylonitrile (**IIb**). Application of the typical procedure using 2-(4-bromophenyl)acetonitrile (0.2 g, 1.02 mmol) and 4-bromobenzaldehyde (0.21 g, 1.12 mmol) gave acrylonitrile **IIb** (0.32 g, 87 %). The spectral data of **IIb** were identical to those reported (Dann et al. 1971).

(Z)-3-(4-Bromophenyl)-2-(4-fluorophenyl)acrylonitrile (**IIc**). Application of the typical procedure using 2-(4-fluorophenyl)acetonitrile (0.2 g, 1.48 mmol) and 4-bromobenzaldehyde (0.3 g, 1.63 mmol) gave

acrylonitrile **IIc** (0.43 g, 96 %). The spectral data of **IIc** were identical to those reported (Csuros et al. 1962).

(Z)-2-(4-Bromophenyl)-3-(4-fluorophenyl)acrylonitrile (**IId**). Application of the typical procedure using 2-(4-bromophenyl)acetonitrile (0.2 g, 1.02 mmol) and 4-fluorobenzaldehyde (0.14 g, 1.12 mmol) gave acrylonitrile **IId** (0.26 g, 85 %). The spectral data of **IId** were identical to those reported (Buu-Hoï et al. 1957).

Synthesis of propanenitriles IIIa-IIId

$NaBH_4$ (1 equiv) was added to a 60-70 °C solution of acrylonitriles **IIa-IId** (1 equiv) in 10 mL of EtOH under a N_2 atmosphere. After stirring for 2.5 h, the reaction was cooled to room temperature and quenched with water. The reaction mixture was acidified with 6 M HCl, extracted with EtOAc (3 × 25 mL), washed with brine, dried over Na_2SO_4, and concentrated in vacuo. The residue was purified by flash chromatography on silica (hexane/EtOAc 9:1) to give propionitriles **IIIa-IIId**.

2,3-Bis(4-fluorophenyl)propanenitrile (**IIIa**). Application of the typical procedure using acrylonitrile **IIa** (0.2 g, 0.83 mmol) gave propanenitrile **IIIa** (0.18 g, 91 %). The spectral data of **IIIa** were identical to those reported (Buschauer et al. 1992).

2,3-Bis(4-bromophenyl)propanenitrile (**IIIb**). Application of the typical procedure using acrylonitrile **IIb** (0.2 g, 0.55 mmol) gave propanenitrile **IIIb** (0.19 g, 95 %). The spectral data of **IIIb** were identical to those reported (Dann et al. 1971).

3-(4-Bromophenyl)-2-(4-fluorophenyl)propanenitrile (**IIIc**). Application of the typical procedure using acrylonitrile **IIc** (0.2 g, 0.66 mmol) gave propanenitrile **IIIc** (0.196 g, 97 %) as a white solid. Chemical purify 93.4% (HPLC). IR (KBr) ν_{max}: 3326, 2928, 2850, 1741, 1610, 1573, 1473 cm^{-1}. ^1H NMR (500 MHz, DMSO-d_6)): δ 7.46 (2H, dm, *J* = 8.4 Hz, Hm'), 7.39 (2H, dd, *J* = 8.8, 5.3 Hz, Ho), 7.20 (2H, dd, *J* = 8.8, 8.8 Hz, Hm), 7.17 (2H, dm, *J* = 8.4 Hz, Ho'), 4.52 (1H, dd, *J* = 7.8, 7.7 Hz, CH), 3.12 (2H, d, *J* = 7.8 Hz, CH_2). ^{13}C NMR δ (188 MHz, DMSO-d_6): 162.1 (d, *J* = 244.3 Hz, Cp), 136.6 (Ci'), 132.1 (d, *J* = 3.0 Hz, Ci), 131.9 (2C, Cm'), 131.6 (2C, Co'), 130.1 (2C, d, *J* = 8.4 Hz, Co), 121.2 (Cp'), 120.7 (CN), 116.2 (2C, d, *J* = 21.6 Hz, Cm), 39.4 (CH_2), 37.2 (CH). ESI-HRMS calculated for $C_{15}H_{11}BrFN$: [M+Na]: 325.995, found: 325.994.

2-(4-Bromophenyl)-3-(4-fluorophenyl)propanenitrile (**IIId**). Application of the typical procedure using acrylonitrile **IId** (0.2 g, 0.66 mmol) gave propanenitrile **IIId** (0.19 g, 94 %). The spectral data of **IIId** were identical to those reported (Jana et al. 2018).

Synthesis of valproic acid derivatives IVa-IVb as HDAC inhibitors

Thionyl chloride $SOCl_2$ (3 mmol) was added dropwise to VPA (3.5 mmol) at 0 °C under a nitrogen atmosphere with constant stirring. The reaction mixture stirred for 1 h under the same conditions and then overnight at room temperature. After this time, Et_3N (0.55 g, 5.45 mmol), the corresponding aniline (2.8 mmol) and 5 mL of hexane were added, and the reaction continued stirring for 3 h. At the end of the

reaction time, 15 mL of EtOAc was added and followed by washing with a saturated $NaHCO_3$ solution (1 × 15 mL) and brine (1 × 15 mL), and the organic phase was dried over anhydrous Na_2SO_4. The solvent was evaporated under reduced pressure, and the residue was purified by column flash chromatography using an eluent mixture of hexane/EtOAc (8:2).

*N-(3-Fluorophenyl)-2-propylpentanamide (***IVa***).* Application of the typical procedure using VPA (0.5 g, 3.5 mmol) and 3-fluoroaniline (0.31 g, 2.8 mmol) gave VPA derivative **IVa** (0.56 g, 85 %). The spectral data of **IVa** were identical to those reported (Muñoz et al. 2020).

*N-(3-methoxyphenyl)-2-propylpentanamide (***IVb***).* Application of the typical procedure using VPA (0.5 g, 3.5 mmol) and 3-methoxyaniline (0.35 g, 2.8 mmol) gave valproic acid derivative **IVb** (0.56 g, 82 %). The spectral data of **IVb** were identical to those reported (Muñoz et al. 2020).

Synthesis of GPER ligands Va-Vd

*(3aS,4S,9bR)-4-(6-Bromobenzo[d][1,3]dioxol-5-yl)-3a,4,5,9b-tetrahydro-3H-cyclopenta[c]quinoline-8-carboxylic acid (***G1-PABA***).* A previous method reported by our research group (Martínez-Muñoz et al. 2018; Zacarias-Lara et al. 2018) was used to obtain G1-PABA. This compound was used as a precursor for the chemical synthesis of GPER ligands **Va-Vd** (Martínez-Muñoz et al. 2018).

Methyl-(3aS,4R,9bR)-4-(6-bromobenzo[d][1,3]dioxol-5-yl)-3a,4,5,9b-tetrahydro-3H-cyclopenta[c]quinoline-8-carboxylate, (**Va**). To a stirred solution of **G1-PABA** (0.25 g, 0.6 mmol) in dry THF (5 mL) and methanol (10 mL) at 0 °C, thionyl chloride (1.32 mL, 1.8 mmol) was added dropwise. The resulting solution was heated to reflux overnight. The solvent and the excess thionyl chloride were then removed under reduced pressure. The resulting crude material was purified by flash chromatography using hexane/EtOAc (8:2) as the eluent, giving the expected product **Va** as a yellow solid (0.23 g, 90 % yield). Full chemical characterization was reported (Zacarias-Lara et al. 2019; Dann et al. 1971).

(3aS,4R,9bR)-4-(6-(3-Methoxyphenyl)benzo[d][1,3]dioxol-5-yl)-3a,4,5,9b-tetrahydro-3H-cyclopenta[c]quinoline-8-carboxylic acid (**Vb**). Compound **Vb** was obtained through a Suzuki Miyaura cross-coupling reaction (Miyaura et al. 1979). A solution of K_2CO_3 (0.27 g, 1.92 mmol) in dimethylformamide (DMF, 5 mL) and water (5 mL) was stirred for 15 min under a N_2 atmosphere. Subsequently, G1-PABA (0.2 g, 0.48 mmol), (3-methoxyphenyl)boronic acid (0.09 g, 0.58 mmol), triphenylphosphine (0.016 g, 0.058 mmol) and $Pd(AcO)_2$ (0.004 g, 0.019 mmol) were added. The reaction mixture was heated to 100 °C for 24 h. Once the reaction was complete, it was allowed to cool to room temperature, and the resulting mixture was extracted with EtOAc (3 × 25 mL). The organic layer was washed with distilled water and brine, dried over anhydrous Na_2SO_4, and concentrated under reduced pressure. Full chemical characterization was reported (Mendéz-Luna D et al 2021 2019).

(3aS,4R,9bR)-4-(6-(3-Nitrophenyl)benzo[d][1,3]dioxol-5-yl)-3a,4,5,9b-tetrahydro-3H-cyclopenta[c]quinoline-8-carboxylic acid (**Vc**). Compound **Vc** was obtained by following a previously reported method (Liu et al. 2005). To a solution of K_2CO_3 (0.27 g, 1.92 mmol) in a 1:1 mixture of $MeOH/H_2O$ (15 mL) with constant

stirring was added G1-PABA (0.2 g, 0.48 mmol), (3-nitrophenyl)boronic acid (0.1 g, 0.58 mmol), PEG2000 (0.060 g, 0.10 mmol) and $Pd(AcO)_2$ (0.004 g, 0.019 mmol) (see Scheme 1). The reaction mixture was heated to reflux at 70 °C for 5 h under a N_2 atmosphere. The solution was then cooled to room temperature, and the resulting mixture was extracted with EtOAc (3×25 mL). The organic phase was washed with distilled water and brine, dried over anhydrous sodium sulfate (Na_2SO_4) and concentrated under reduced pressure. The residue was purified by flash chromatography using a mixture of hexane/EtOAc (7:3) as the eluent. Full chemical characterization was reported (Mendéz-Luna D et al 20212019).

(3aS,4R,9bR)-4-(6-Bromobenzo[d][1,3]dioxol-5-yl)-5-(tert-butoxycarbonyl)-3a,4,5,9b-tetrahydro-3H-cyclopenta[c]quinoline-8-carboxylic acid (**Vd**). To a cold solution of G1-PABA in DMF (3.0 mL), triethylamine (336 µL, 2.4 mmol) was added dropwise with continuous stirring for 30 min at the same temperature. Subsequently, di-tert-butyl dicarbonate (Boc_2O, 0.53 g, 2.4 mmol) was added, and the reaction mixture was allowed to reach room temperature and continued overnight with vigorous stirring. The progress of the reaction was monitored by TLC, and the resulting mixture was extracted with EtOAc (3 × 25 mL). The organic phase was washed with water and brine, dried over anhydrous Na_2SO_4 and evaporated to dryness. The residue obtained was purified by flash chromatography using a mobile phase of hexane/EtOAc (9:1). Full chemical characterization was reported (Mendéz-Luna D et al 20212019).

Synthesis of hydroxamic derivatives VIa-VIg

4-Butyl-N-(2-(hydroxyamino)-2-oxoethyl)benzamide (**VIa**). The procedure started with 0.12 mmol of resin, HATU (0.18 g, 0.48 mmol), HOAt (0.066 g, 0.48 mmol), DIPEA (84 µL, 0.48 mmol), Fmoc-glycine (0.144 g, 0.48 mmol) and 4-butylbenzoic acid (0.086 g, 0.48 mmol). The resulting compound was purified by flash chromatography using EtOAc/MeOH/MeCN/H_2O as the mobile phase (70/2.5/1.25/1.25). A white solid was obtained (0.008 g, 26 %). Full chemical characterization was reported (Sixto-Lopez et al. 2020).

(S)-N-(1-(Hydroxyamino)-1-oxo-3-phenylpropan-2-yl)-2-propylpentanamide (**VIb**). The procedure was followed starting with 0.12 mmol of resin, HATU (0.19 g, 0.50 mmol), HOAt (0.068 g, 0.50 mmol), DIPEA (87 µL, 0.50 mmol), Fmoc-L-phenylalanine (0.192 g, 0.50 mmol) and valproic acid (0.072 g, 0.50 mmol). The resulting compound was purified by recrystallization from DCM. A white solid was obtained (0.013 g, 36 %). Full chemical characterization was reported (Sixto-Lopez et al. 2020).

(R)-4-Butyl-N-(1-(hydroxyamino)-1-oxo-3-phenylpropan-2-yl)benzamide (**VIc**). The procedure was followed starting with 0.14 mmol of resin, DIC (57 µL, 0.57 mmol), HOAt (0.078 g, 0.57 mmol), Fmoc-D-phenylalanine (1.22 g, 0.57 mmol) and 4-butylbenzoic acid (0.102 g, 0.57 mmol). The compound was purified by recrystallization from DCM. A white solid was obtained (0.025 g, 51 %). Full chemical characterization was reported (Sixto-Lopez 2013).

(S)-4-Butyl-N-(1-(hydroxyamino)-3-(naphthalen-2-yl)-1-oxopropan-2-yl)benzamide (**VId**). The procedure was followed starting with 0.14 mmol of resin, DIC (57 µL, 0.57 mmol), HOAt (0.078 g, 0.57 mmol), Fmoc-

3-(2-naphthyl)-L-alanine (0.251 g, 0.57 mmol) and 4-butylbenzoic acid (0.102 g, 0.57 mmol). The resulting compound was purified by recrystallization from DCM. A white solid was obtained (0.039 g, 70 %). Full chemical characterization was reported (Sixto-Lopez et al. 2020).

(S)-4-Butyl-N-(3-(4-fluorophenyl)-1-(hydroxyamino)-1-oxopropan-2-yl)benzamide (**VIe**). The procedure was followed starting with 0.14 mmol of resin, DIC (57 µL, 0.57 mmol), HOAt (0.078 g, 0.57 mmol), Fmoc-L-Phe(4-F)-OH (0.232 g, 0.57 mmol) and 4-butylbenzoic acid (0.102 g, 0.57 mmol). The compound was purified by flash chromatography using EtOAc/MeOH/MeCN/H_2O as the mobile phase (70/2.5/1.25/1.25). A salmon colored solid was obtained (0.102 g, 43 %). Full chemical characterization was reported (Sixto-Lopez et al. 2020).

(S)-4-Butyl-N-(1-(hydroxyamino)-3-(4-iodophenyl)-1-oxopropan-2-yl)benzamide (**VIf**). The procedure was followed starting with 0.14 mmol of resin, DIC (57 µL, 0.57 mmol), HOAt (0.078 g, 0.57 mmol), Fmoc-L-Phe(4-I)-OH (0.294 g, 0.57 mmol) and 4-butylbenzoic acid (0.102 g, 0.57 mmol). The compound was purified by recrystallization from DCM. A white solid was obtained (0.044 g, 66 %). Full chemical characterization was reported (Sixto-Lopez 2013).

(S)-4-Butyl-N-(1-(hydroxyamino)-3-(4-nitrophenyl)-1-oxopropan-2-yl)benzamide (**VIg**). The procedure was followed starting with 0.14 mmol of resin, DIC (57 µL, 0.57 mmol), HOAt (0.078 g, 0.57 mmol), Fmoc-L-Phe(4-NO_2)-OH (0.248 g, 0.57 mmol) and 4-butylbenzoic acid (0.102 g, 0.57 mmol). The compound was purified by flash chromatography using EtOAc/MeOH/MeCN/H_2O as the mobile phase (70/2.5/1.25/1.25). A white solid was obtained (0.03 g, 60 %). Full chemical characterization was reported (Sixto-Lopez et al. 2020).

Biological evaluation

Cell culture

Isolation and culture of GBM cells using the classical nonadherent neurospheres (NS) method was performed according to a protocol used to derive NS from the adult human spinal cord as described by Dromard et al. (Dromard et al. 2008) and adapted by Guichet et al. for Gli4 cells (Guichet et al. 2013). In proliferation condition when GBM cells form NS, cells were cultivated in DMEM/F12 medium supplemented with glucose, glutamine, insulin, N2, Epidermal Growth Factor and Fibroblast Growth Factor, (proliferation medium). For migration, GSCs cell culture was realized in DMEM/F12 medium supplemented with glucose, glutamine, insulin, N2 and fetal bovine serum (0.5%). Prior to cell seeding, 2D or NF were either functionalized or not with poly-D-lysine added overnight and then the addition of LN (sigma L2020) (0.05mg/mL) 1 h at 37°C.

For migration assay, same size GBM NS were performed by seeding 5000 cells in round bottom wells and remained in culture during 2 days until formation of single neurosphere due to sedimentation. Compounds were prepared in 100% DMSO and diluted in media to obtain in each condition a final

percentage of 0.3% DMSO. Then GSCs NS were deposited on the top of NF +LN and let to migrate during 5 days in total, with 72 h in presence of either HDAC compounds or 0.3% DMSO alone for control.

Immunofluorescence: GSCs cultures were fixed by 4% PFA. Cell and brain sections were blocked and permeabilized using PBS - triton 0.5% - horse serum 5%. Fluorochrome-coupled phalloidin 546 was incubated 2 h at room temperature (dilution 1/500). Image acquisition was realized using Zeiss Axioimager Z1/ Zen (with an apotome). Migration quantifications were done using ZEN 2012 sotfware, migration capacity was quantified by measuring an area of migration. To measure migration areas, we subtracted the area of the NS containing non-migrating cells from the total area where cells were detected.

Antiproliferativeactivity: MTT assay

The GBM stem cells are primary cell culture coming from patient, gently donate by Luc Bauchet from the Hospital Guy de Chauliac and isolated by the Professor Jean-Philippe Hugnot *(Guichet et al. 2013; Saleh et al. 2019).* Gli4 were seeded into 96-well plates at 3000 cells per well in a 2D system and 15000 cells in a 3D system, 2D culture were culture with laminin (2D+LN) or without laminin (2D-LN), while 3D systems were also culture with laminin (3D+LN) as single cells or without laminin (3D-LN) for collective migrations. Once the cells were adherent, different concentration of the compound were added at the µM range (Table 1) to each well at a final DMSO concentration of 0.3 %, Phostine (PST3) was testes as positive control at 1 µM in 0.3% DMSO. The MTT assay was carried out as previously described 72 h after the addition of compounds (Mosmann 1983). Active compounds were tested in four independent experiments, and each experiment was carried out in triplicate for each condition.

Statistical analyses

The experiments were carried out at least in triplicate, depending on the number of independent variables. Student's or ANOVA statistical tests were applied using Serf software (bram.org/serf/CellsAndMaps.php) and GraphPad. EC_{50} and Ki values were calculated using the Hill equation from the dose–log response curves.

Results And Discussion

Cancer cells are presenting numerous deregulation favoring the overexpression of several proteins which could be a target for drug design as GPER1 (Martínez-Muñoz et al. 2018; Zacarias-Lara OJ, et al. 2018) leading to cell proliferation and migration. GBM is a disease with a poor survival rate and limited therapeutic options. Therefore, a multitargeted approach for drug screening is necessary in order to explore several pharmacological options for GBM treatment (Shea et al. 2016). Traditional 2D cell cultures (monolayers) are widely used to assay antiproliferative activity as one of the first approaches to decide if a compound should be further investigated as an anticancer drug (Shan et al. 2018; Verjans et al. 2018). However, it is well admitted that the use of this strategy is the cause of the failure to discover new anticancer drugs because 2D cell cultures not mimic the *in vivo* 3D fibrillar microenvironment, cell-

cell interactions, and cell-extracellular matrix interactions (Lv et al. 2017). Therefore, 3D cultures may be a powerful tool for drug discovery, offering a more realistic approach for drug screening (Lv et al. 2017). Our group has previously focused is work on drug design employing *in silico* tools (Zacarias-Lara et al. 2019; Sixto-Lopez et al. 2020). In this drug screening preliminary study, compounds are chemically synthesized targeting the 24 candidates potentially able to impair proliferative and migrating behaviour of GSCs (Zacarias-Lara et al. 2019; Sixto-Lopez et al. 2020). (Rajak et al. 2013; Wang 2009; Lan et al. 2017; Batistatou et al. 2004; Wan et al. 2018; Liu et al. 2018; Zhou et al. 2019; Martinez-Archundia et al. 2018; Feldman and Limbird 2017; Meitzler et al. 2014; Munson et al. 2013; Nayernia et al. 2014). Those targeted proteins are tackling several pathways, including HDACs leading to epigenetic modulation, ROS production and GPER and ER modulators associated in multiple cancer with cell proliferation and metastasis. First, to evaluate the potential anti proliferative effect of the compounds, we performed MTT test on GSC in 2D and 3D with or without LN by adding the different compounds during 72h. During this first screening, the following compounds (from the Table 1) appeared unefficient on the GSC for the : NADPH oxidase inhibitors **Ia**-**Ib**, estrogen receptor modulators **IId** and **IIIa**-**IIId**, valproic acid derivatives **IVa**-**IVb**, GPER ligands **Va**-**Vd** and two hydroxamic acid derivatives **VIa** and **VIg** (Table 1). Those compounds didn't present any cytotoxic or antiproliferative potential. Nevertheless, five HDACis hydroxamic acid derivatives (**VIb-VIf**), exhibited equal antiproliferative efficiency on GSC either in 2D or in 3D. The assays were performed in presence and absence of laminin, in order to recapitulate collective and individual migration mode (Saleh et al. 2019). The anti proliferative effect of the compounds (**VIb-VIf**) targeting HDACs didn't present any specificity against single or collective migratory cells (Table 2) (Fig. 1D). ERβ, here targeted by the compounds IIa, has been described in other studies as inhibiting the proliferation of glioma cell lines (Sareddy et al. 2016). However, the estrogen modulator IIa seems to present anti proliferative properties in 2D, but not in 3D, validating the 3D model choice as stringent drug screening model for candidate selection

The HDAC antiproliferative effects is also already well described(Was et al. 2019; Li et al. 2015). For instance, HDAC8 inhibition by a specific inhibitor produces DNA damage, cell cycle arrest and decreases cell viability and thoseeffects were associated with the inhibition of the O^6-methyl-guanine DNA methyltransferase (Santos-Barriopedro et al. 2019). In its turn, HDAC6 inhibition decreases GBM cell growth due to of SMAD2 phosphorylation inhibition and down expression regulation of p21 (Li et al. 2015).

HDACi (VIb-VIf) were previously designed and synthesized depicting antiproliferative properties against a panel of cancer cell line such as, hepatocellular carcinoma (HepG2), pancreatic cancer (MIA PaCa-2), breast cancer (MCF-7 and HCC1954), renal cancer (RCC4-VHL and RCC4-VA) and neuroblastoma (SH-SY5Y). According to molecular docking and MD simulations studies, these compounds might block the catalytic cavity of HDAC1, HDAC6 and HDAC8, which could be due to their aromatic portion that is able to interact with residues surrounding the catalytic tunnel (Sixto-Lopez et al. 2020). Therefore, due to the previous promissory activity against several cancer cell lines, these HDACic were tested against GBM cell lines in order to explore the antiproliferative and antimigratory activity against this disease.

GSCs during migration start differentiation process, hence decreasing proliferation capacity. As HDACs compounds are described as targeting proliferation, also following the proliferation assay for the compounds (VIb-VIf), we decided to evaluate HDACs inhibitor effects on migration (Fig. 1A, B) and then potential impairment of cell viability. We deposited same size neurosphere (NS) (5000 GSCs) on those 3D matrices with LN, leave them to migrate during 5days and applied treatment during 72h, and quantified the NS size and the migration area around the NS after subtracting the NS area from the total migration (Fig. 1C). The HDACs inhibitor compounds (VIb-VIf), appear as not decreasing the migrating capacity of the GSC comparing to the control condition. We can hypothesize that HDACs hydroxamic acid derivatives are not cytotoxic but impair proliferation capacity without impairing migration in 3D fibrillar matrix. Also, the compounds VIe and VIf show only NS size decrease after 72h treatment illustrating the antiproliferative effect of the HDACs, independently of a potential anti-migration effect. Following those preliminary experiment and for upcoming studies we have, on first hand, to evaluate EC50 of the HDACs hydroxamic acid derivatives and, on the other hand, evaluate *in vivo* efficiency of those compounds, potential cytotoxicity and side effects. In fact, HDACs, are well describe as having great therapeutic potential but also pleiotropic effects at the cellular and systemic levels and seems to present ability to modulate the immune system affecting many cellular functions. Indeed, their use is recently extended far beyond cancer treatment in terms of their therapeutic capacity (Hull et al. 2016). Consequently, it seems essential to perform *in vivo* trials as next step for those HDACs inhibitor potential evaluation and ultimate determine their action mechanism.

Conclusion

In this study, we are evaluating the efficiency of 24 compounds targeting some deregulated proteins described as improving cancer proliferation (including HDACs, GPER and Erβ modulators, NADPH oxidase inhibitor), therefore, impairing patient survival. Among those 24 compounds, according to proliferation and migration assay results in 2D and 3D, we selected HDACs inhibitor compounds (**VIb-VIf**) as possible candidate for *in vivo* trial in order to evaluate their anti tumoral efficiency and potential toxicity.

Declarations

Availability of data and material: Not applicable

Code availability: Not applicable.

Author Contribution: YSL, wrote the manuscript and synthetized HDACi; EM, performed cell culture; JBGV, synthetize compounds and wrote the manuscript; JFV, Synthetized and analysis compounds; MCRH synthetized compounds, wrote paper; OZL synthetized and analyze compound; DML, synthetized compounds, JAGV synthetized and analyzed HDACi; DC, performed biological assays; BN, design project and wrote the manuscript; JBC, design project and wrote the manuscript.

Funding information: We gratefully acknowledge to CONACYT (Grants: CB-254600, APN-782 and SEP-CONACYT-ANUIES-ECOS Francia: 296636), to Instituto Politécnico Nacional (Grant: Proyectos Insignia IPN-2015), and to COFAA-SIP/IPN.

Compliance with ethical standards

Conflict of interest None conflicts of interest are present for any of the authors.

Ethics approval This article does not contain any studies with human participants performed by any of the authors.

Consent to participate: Not applicable.

Consent for publish: Not applicable.

Acknowledgments

Y.S.L. thanks to CONACYT for PhD scholarship.

References

Batistatou A, Stefanou D, Goussia A, Arkoumani E, Papavassiliou AG, Agnantis NJ (2004) Estrogen receptor beta (ERbeta) is expressed in brain astrocytic tumors and declines with dedifferentiation of the neoplasm. J Cancer Res Clin Oncol 130 (7):405-410. doi:10.1007/s00432-004-0548-9

Buschauer A, Friese-Kimmel A, Baumann G, Schunack W (1992) Synthesis and histamine H2 agonistic activity of arpromidine analogues: replacement of the pheniramine-like moiety by non-heterocyclic groups. European Journal of Medicinal Chemistry 27 (4):321-330. doi:10.1016/0223-5234(92)90145-q

Buu-HoÏ NP, Xuong ND, Rips R (1957) New Fluorine-containing Aromatics as Potential Carcinostats. The Journal of Organic Chemistry 22 (2):193-197. doi:10.1021/jo01353a028

Csuros Z, Deak G, Szolnoki J (1962) Condensation of benzaldehyde and benzyl cyanide catalyzed by ion exchange resins. Preparation of some new ring-substituted α-phenylcinnamonitrile derivatives. . Acta Chimica Academiae Scientiarum Hungaricae 33 (1):341-342

Dann O, Bergen G, Demant E, Volz G (1971) Trypanocide Diamidine des 2-Phenyl-benzofurans, 2-Phenyl-indens und 2-Phenyl-indols. Justus Liebigs Annalen der Chemie 749 (1):68-89. doi:10.1002/jlac.19717490110

Dromard C, Guillon H, Rigau V, Ripoll C, Sabourin JC, Perrin FE, Scamps F, Bozza S, Sabatier P, Lonjon N, Duffau H, Vachiery-Lahaye F, Prieto M, Tran Van Ba C, Deleyrolle L, Boularan A, Langley K, Gaviria M, Privat A, Hugnot JP, Bauchet L (2008) Adult human spinal cord harbors neural precursor cells that

generate neurons and glial cells in vitro. Journal of neuroscience research 86 (9):1916-1926. doi:10.1002/jnr.21646

Feldman RD, Limbird LE (2017) GPER (GPR30): A Nongenomic Receptor (GPCR) for Steroid Hormones with Implications for Cardiovascular Disease and Cancer. Annu Rev Pharmacol Toxicol 57:567-584. doi:10.1146/annurev-pharmtox-010716-104651

Guichet PO, Bieche I, Teigell M, Serguera C, Rothhut B, Rigau V, Scamps F, Ripoll C, Vacher S, Taviaux S, Chevassus H, Duffau H, Mallet J, Susini A, Joubert D, Bauchet L, Hugnot JP (2013) Cell death and neuronal differentiation of glioblastoma stem-like cells induced by neurogenic transcription factors. Glia 61 (2):225-239. doi:10.1002/glia.22429

Hull EE, Montgomery MR, Leyva KJ (2016) HDAC Inhibitors as Epigenetic Regulators of the Immune System: Impacts on Cancer Therapy and Inflammatory Diseases. BioMed research international 2016:8797206. doi:10.1155/2016/8797206

Hsieh CH, Wu CP, Lee HT, Liang JA, Yu CY, Lin YJ (2012) NADPH oxidase subunit 4 mediates cycling hypoxia-promoted radiation resistance in glioblastoma multiforme. Free radical biology & medicine 53 (4):649-658. doi:10.1016/j.freeradbiomed.2012.06.009

Jana A, Reddy CB, Maji B (2018) Manganese Catalyzed α-Alkylation of Nitriles with Primary Alcohols. ACS Catalysis 8 (10):9226-9231. doi:10.1021/acscatal.8b02998

Kim RK, Kim MJ, Yoon CH, Lim EJ, Yoo KC, Lee GH, Kim YH, Kim H, Jin YB, Lee YJ, Cho CG, Oh YS, Gye MC, Suh Y, Lee SJ (2012) A new 2-pyrone derivative, 5-bromo-3-(3-hydroxyprop-1-ynyl)-2H-pyran-2-one, suppresses stemness in glioma stem-like cells. Molecular pharmacology 82 (3):400-407. doi:10.1124/mol.112.078402

Lan YL, Zou S, Wang X, Lou JC, Xing JS, Yu M, Zhang B (2017) Update on the therapeutic significance of estrogen receptor beta in malignant gliomas. Oncotarget 8 (46):81686-81696. doi:10.18632/oncotarget.20970

Lee DH, Ryu HW, Won HR, Kwon SH (2017) Advances in epigenetic glioblastoma therapy. Oncotarget 8 (11):18577-18589. doi:10.18632/oncotarget.14612

Li S, Liu X, Chen X, Zhang L, Wang X (2015) Histone deacetylase 6 promotes growth of glioblastoma through inhibition of SMAD2 signaling. Tumour Biol 36 (12):9661-9665. doi:10.1007/s13277-015-3747-x

Liu G, Yuan X, Zeng Z, Tunici P, Ng H, Abdulkadir IR, Lu L, Irvin D, Black KL, Yu JS (2006) Analysis of gene expression and chemoresistance of CD133+ cancer stem cells in glioblastoma. Molecular cancer 5:67. doi:10.1186/1476-4598-5-67

Liu J, Sareddy GR, Zhou M, Viswanadhapalli S, Li X, Lai Z, Tekmal RR, Brenner A, Vadlamudi RK (2018) Differential Effects of Estrogen Receptor beta Isoforms on Glioblastoma Progression. Cancer Res 78

(12):3176-3189. doi:10.1158/0008-5472.CAN-17-3470

Liu L, Zhang Y, Wang Y (2005) Phosphine-free palladium acetate catalyzed Suzuki reaction in water. The Journal of organic chemistry 70 (15):6122-6125. doi:10.1021/jo050724z

Lv D, Hu Z, Lu L, Lu H, Xu X (2017) Three-dimensional cell culture: A powerful tool in tumor research and drug discovery. Oncology letters 14 (6):6999-7010. doi:10.3892/ol.2017.7134

Macias Perez ME, Hernandez Rodriguez M, Cabrera Perez LC, Fragoso-Vazquez MJ, Correa-Basurto J, Padilla M, II, Mendez Luna D, Mera Jimenez E, Flores Sandoval C, Tamay Cach F, Rosales-Hernandez MC (2017) Aromatic Regions Govern the Recognition of NADPH Oxidase Inhibitors as Diapocynin and its Analogues. Archiv der Pharmazie 350 (10). doi:10.1002/ardp.201700041

Martinez-Archundia M, Garcia-Vazquez JB, Colin-Astudillo B, Bello M, Prestegui-Martel B, Chavez-Blanco A, Duenas-Gonzalez A, Fragoso-Vazquez MJ, Mendieta-Wejebe J, Abarca-Rojano E, Ordaz-Rosado D, Garcia-Becerra R, Castillo-Bautista D, Correa Basurto J (2018) Computational Study of the Binding Modes of Diverse DPN Analogues on Estrogen Receptors (ER) and the Biological Evaluation of a New Potential Antiestrogenic Ligand. Anticancer Agents Med Chem 18 (11):1508-1520. doi:10.2174/1871520618666171129152953

Martinez-Munoz A, Prestegui-Martel B, Mendez-Luna D, Fragoso-Vazquez MJ, Garcia-Sanchez JR, Bello M, Martinez-Archundia M, Chavez-Blanco A, Duenas-Gonzalez A, Mendoza-Lujambio I, Trujillo-Ferrara J, Correa-Basurto J (2018) Selection of a GPER1 Ligand via Ligand-based Virtual Screening Coupled to Molecular Dynamics Simulations and Its Anti-proliferative Effects on Breast Cancer Cells. Anti-cancer agents in medicinal chemistry 18 (11):1629-1638. doi:10.2174/1871520618666180510121431

Meitzler JL, Antony S, Wu Y, Juhasz A, Liu H, Jiang G, Lu J, Roy K, Doroshow JH (2014) NADPH oxidases: a perspective on reactive oxygen species production in tumor biology. Antioxidants & redox signaling 20 (17):2873-2889. doi:10.1089/ars.2013.5603

Mendéz-Luna D (2019) Rational in silico design, chemical synthesis and in vitro evaluation of new ligands targeting the GPER1 / GPR30 receptor with possible anti-cancer activity. Insituto Politécnico Nacional, Mexico

Méndez-Luna D, Morelos-Garnica LA, García-Vázquez JB, Bello M, Padilla-Martínez II, Fragoso-Vázquez MJ, Dueñas González A, De Pedro N, Gómez-Vidal JA, Mendoza-Figueroa HL, Correa-Basurto J. Modifications on the Tetrahydroquinoline Scaffold Targeting a Phenylalanine Cluster on GPER as Antiproliferative Compounds against Renal, Liver and Pancreatic Cancer Cells. Pharmaceuticals (Basel). 2021 Jan 10;14(1):49. doi: 10.3390/ph14010049.

Miyaura N, Yamada K, Suzuki A (1979) A new stereospecific cross-coupling by the palladium-catalyzed reaction of 1-alkenylboranes with 1-alkenyl or 1-alkynyl halides. Tetrahedron Letters 20 (36):3437-3440. doi:10.1016/s0040-4039(01)95429-2

Mosmann T (1983) Rapid colorimetric assay for cellular growth and survival: Application to proliferation and cytotoxicity assays. Journal of Immunological Methods 65 (1-2):55-63. doi:10.1016/0022-1759(83)90303-4

Munoz AM, Fragoso-Vazquez MJ, Martel BP, Chavez-Blanco A, Duenas-Gonzalez A, Garcia-Sanchez JR, Bello M, Romero-Castro A, Correa-Basurto J (2020) Targeting Breast Cancer Cells with G4 PAMAM Dendrimers and Valproic Acid Derivative Complexes. Anticancer Agents Med Chem. doi:10.2174/1871520620666200423073812

Munson J, Bonner M, Fried L, Hofmekler J, Arbiser J, Bellamkonda R (2013) Identifying new small molecule anti-invasive compounds for glioma treatment. Cell cycle 12 (14):2200-2209. doi:10.4161/cc.25334

Nakada M, Kita D, Watanabe T, Hayashi Y, Teng L, Pyko IV, Hamada J (2011) Aberrant signaling pathways in glioma. Cancers 3 (3):3242-3278. doi:10.3390/cancers3033242

Nayernia Z, Jaquet V, Krause KH (2014) New insights on NOX enzymes in the central nervous system. Antioxidants & redox signaling 20 (17):2815-2837. doi:10.1089/ars.2013.5703

Rajak H, Singh A, Raghuwanshi K, Kumar R, Dewangan PK, Veerasamy R, Sharma PC, Dixit A, Mishra P (2013) A Structural Insight into Hydroxamic Acid Based Histone Deacetylase Inhibitors for the Presence of Anticancer Activity. Current Medicinal Chemistry 21 (23):2642-2664. doi:10.2174/09298673113209990191

Saleh A, Marhuenda E, Fabre C, Hassani Z, Weille J, Boukhaddaoui H, Guelfi S, Maldonado IL, Hugnot JP, Duffau H, Bauchet L, Cornu D, Bakalara N (2019) A novel 3D nanofibre scaffold conserves the plasticity of glioblastoma stem cell invasion by regulating galectin-3 and integrin-beta1 expression. Scientific reports 9 (1):14612. doi:10.1038/s41598-019-51108-w

Santos-Barriopedro I, Li Y, Bahl S, Seto E (2019) HDAC8 affects MGMT levels in glioblastoma cell lines via interaction with the proteasome receptor ADRM1. Genes Cancer 10 (5-6):119-133. doi:10.18632/genesandcancer.197

Sareddy GR, Li X, Liu J, Viswanadhapalli S, Garcia L, Gruslova A, Cavazos D, Garcia M, Strom AM, Gustafsson JA, Tekmal RR, Brenner A, Vadlamudi RK (2016) Selective Estrogen Receptor beta Agonist LY500307 as a Novel Therapeutic Agent for Glioblastoma. Sci Rep 6:24185. doi:10.1038/srep24185

Shan F, Close DA, Camarco DP, Johnston PA (2018) High-Content Screening Comparison of Cancer Drug Accumulation and Distribution in Two-Dimensional and Three-Dimensional Culture Models of Head and Neck Cancer. Assay and drug development technologies 16 (1):27-50. doi:10.1089/adt.2017.812

Shea A, Harish V, Afzal Z, Chijioke J, Kedir H, Dusmatova S, Roy A, Ramalinga M, Harris B, Blancato J, Verma M, Kumar D (2016) MicroRNAs in glioblastoma multiforme pathogenesis and therapeutics. Cancer

medicine 5 (8):1917-1946. doi:10.1002/cam4.775

Singh SK, Hawkins C, Clarke ID, Squire JA, Bayani J, Hide T, Henkelman RM, Cusimano MD, Dirks PB (2004) Identification of human brain tumour initiating cells. Nature 432 (7015):396-401. doi:10.1038/nature03128

Sixto-Lopez Y (2013) Computational design, synthesis and biological evaluation of bifunctional histone deacetylase 8 and 6 inhibitors with double action at the catalytic and hydrophobic site. Instituto Politécnico Nacional,

Sixto-Lopez Y, Gómez-Vidal JA, de Pedro N, Bello M, Rosales-Hernandez MC, Correa-Basurto J (2020) Hydroxamic acid derivatives as HDAC1, HDAC6 and HDAC8 inhibitors with antiproliferative activity in cancer cell lines. Scientific reports:18. doi:https://doi.org/10.1038/s41598-020-67112-4

Vaccaro W, Amore C, Berger J, Burrier R, Clader J, Davis H, Domalski M, Fevig T, Salisbury B, Sher R (1996) Inhibitors of acyl CoA:cholesterol acyltransferase. Journal of medicinal chemistry 39 (8):1704-1719. doi:10.1021/jm950833d

Vegeto E, Belcredito S, Etteri S, Ghisletti S, Brusadelli A, Meda C, Krust A, Dupont S, Ciana P, Chambon P, Maggi A (2003) Estrogen receptor-alpha mediates the brain antiinflammatory activity of estradiol. Proceedings of the National Academy of Sciences of the United States of America 100 (16):9614-9619. doi:10.1073/pnas.1531957100

Verjans ET, Doijen J, Luyten W, Landuyt B, Schoofs L (2018) Three-dimensional cell culture models for anticancer drug screening: Worth the effort? Journal of cellular physiology 233 (4):2993-3003. doi:10.1002/jcp.26052

Wan S, Jiang J, Zheng C, Wang N, Zhai X, Fei X, Wu R, Jiang X (2018) Estrogen nuclear receptors affect cell migration by altering sublocalization of AQP2 in glioma cell lines. Cell death discovery 4:49. doi:10.1038/s41420-018-0113-y

Wan S, Jiang J, Zheng C, Wang N, Zhai X, Fei X, Wu R, Jiang X (2018) Estrogen nuclear receptors affect cell migration by altering sublocalization of AQP2 in glioma cell lines. Cell death discovery 4:49. doi:10.1038/s41420-018-0113-y

Wang D (2009) Computational Studies on the Histone Deacetylases and the Design of Selective Histone Deacetylase Inhibitors. *Current Topics in Medicinal Chemistry* 9 (3):241-256. doi:10.2174/156802609788085287

Was H, Krol SK, Rotili D, Mai A, Wojtas B, Kaminska B, Maleszewska M (2019) Histone deacetylase inhibitors exert anti-tumor effects on human adherent and stem-like glioma cells. Clin Epigenetics 11 (1):11. doi:10.1186/s13148-018-0598-5

Yang CC, Hsiao LD, Tseng HC, Kuo CM, Yang CM (2020) Pristimerin Inhibits MMP-9 Expression and Cell Migration Through Attenuating NOX/ROS-Dependent NF-kappaB Activation in Rat Brain Astrocytes Challenged with LPS. Journal of inflammation research 13:325-341. doi:10.2147/JIR.S252659

Yelton CJ, Ray SK (2018) Histone deacetylase enzymes and selective histone deacetylase inhibitors for antitumor effects and enhancement of antitumor immunity in glioblastoma. Neuroimmunology and neuroinflammation 5. doi:10.20517/2347-8659.2018.58

Zacarias-Lara OJ, Mendez-Luna D, Martinez-Ruiz G, Garcia-Sanchez JR, Fragoso-Vazquez MJ, Bello M, Becerra-Martinez E, Garcia-Vazquez JB, Correa-Basurto J (2018) Synthesis and In Vitro Evaluation of Tetrahydroquinoline Derivatives as Antiproliferative Compounds of Breast Cancer via Targeting The GPER. Anti-cancer agents in medicinal chemistry. doi:10.2174/1871520618666181119094144

Zacarias-Lara OJ, Mendez-Luna D, Martinez-Ruiz G, Garcia-Sanchez JR, Fragoso-Vazquez MJ, Bello M, Becerra-Martinez E, Garcia-Vazquez JB, Correa-Basurto J (2019) Synthesis and In Vitro Evaluation of Tetrahydroquinoline Derivatives as Antiproliferative Compounds of Breast Cancer via Targeting the GPER. Anticancer Agents Med Chem 19 (6):760-771. doi:10.2174/1871520618666181119094144

Zhou M, Sareddy GR, Li M, Liu J, Luo Y, Venkata PP, Viswanadhapalli S, Tekmal RR, Brenner A, Vadlamudi RK (2019) Estrogen receptor beta enhances chemotherapy response of GBM cells by down regulating DNA damage response pathways. Sci Rep 9 (1):6124. doi:10.1038/s41598-019-42313-8

Tables

Table 1. Percent inhibition of cell proliferation of the tested compounds obtained in 2D and 3D GBM cell cultures with or without laminin.

Compound		% Inhibition			
	Concentration tested (µM)	2D-LN	3D-LN	2D+LN	3D+LN
Ia	10	7.030	18.388	-9.329	-25.771
Ib	10	-4.419	14.857	8.04	3.699
IIa*	10	56.301	36.828	68.923	53.692
IIb	10	-91.405	32.654	-24.236	8.607
IIc	10	-38.858	14.843	-31.901	3.179
IId	10	-29.136	3.223	8.204	-17.542
IIIa	10	-11.432	23.33	10.269	-22.214
IIIb	10	-27.736	10.921	5.391	13.261
IIIc	10	-12.795	24.519	9.829	-24.944
IIId	10	19.213	37.053	7.376	-35.252
IVa	42	3.205	-25.811	37.878	37.193
IVb	40	4.8559	-7.297	2.518	11.854
Va	23	11.724	18.861	-42.666	6.772
Vb	22	-11.233	23.972	-21.05	1.157
Vc	22	-22.627	-106.95	-16.014	10.793
Vd	19	2.733	-80.941	1.617	-1.717
VIa	40	-12.222	-11.288	8.746	7.809
VIb*	32	63.066	28.205	68.872	61.086
VIc*	29	48.657	51.541	62.955	47.845
VId*	26	58.91	45.936	56.7	56.946
VIe*	28	48.143	41.135	47.099	54.078
VIf*	21	55.017	41.902	55.994	44.821
VIg	26	-2.397	-11.020	31.680	-16.718
Phostine*	1	56.517	10.591	70.898	65.767

* These compounds were selected for a second test. In the table, the indicated value represents the average of the first and second experiments.

Note: 2D-LN= 2D cell culture without laminin; 2D+LN= 2D cell culture with laminin; 3D-LN= 3D cell culture without laminin; 3D+LN= 3D cell culture with laminin

Table 2. Final list of compounds that showed antiproliferative activity in 2D and 3D GBM cell cultures with or without laminin.

Compound	% Inhibition			
	2D-LN	3D-LN	2D+LN	3D+LN
IIa	56.301	36.828	68.923	53.692
VIb	63.066	28.205	68.872	61.086
VIc	48.657	51.541	62.955	47.845
VId	58.91	45.936	56.7	56.946
VIe	48.143	41.135	47.099	54.078
VIf	55.017	41.902	55.994	44.821
Phostine	56.517	10.591	70.898	65.767

Note: 2D-LN= 2D cell culture without laminin; 2D+LN= 2D cell culture with laminin; 3D-LN= 3D cell culture without laminin; 3D+LN= 3D cell culture with laminin

Figures

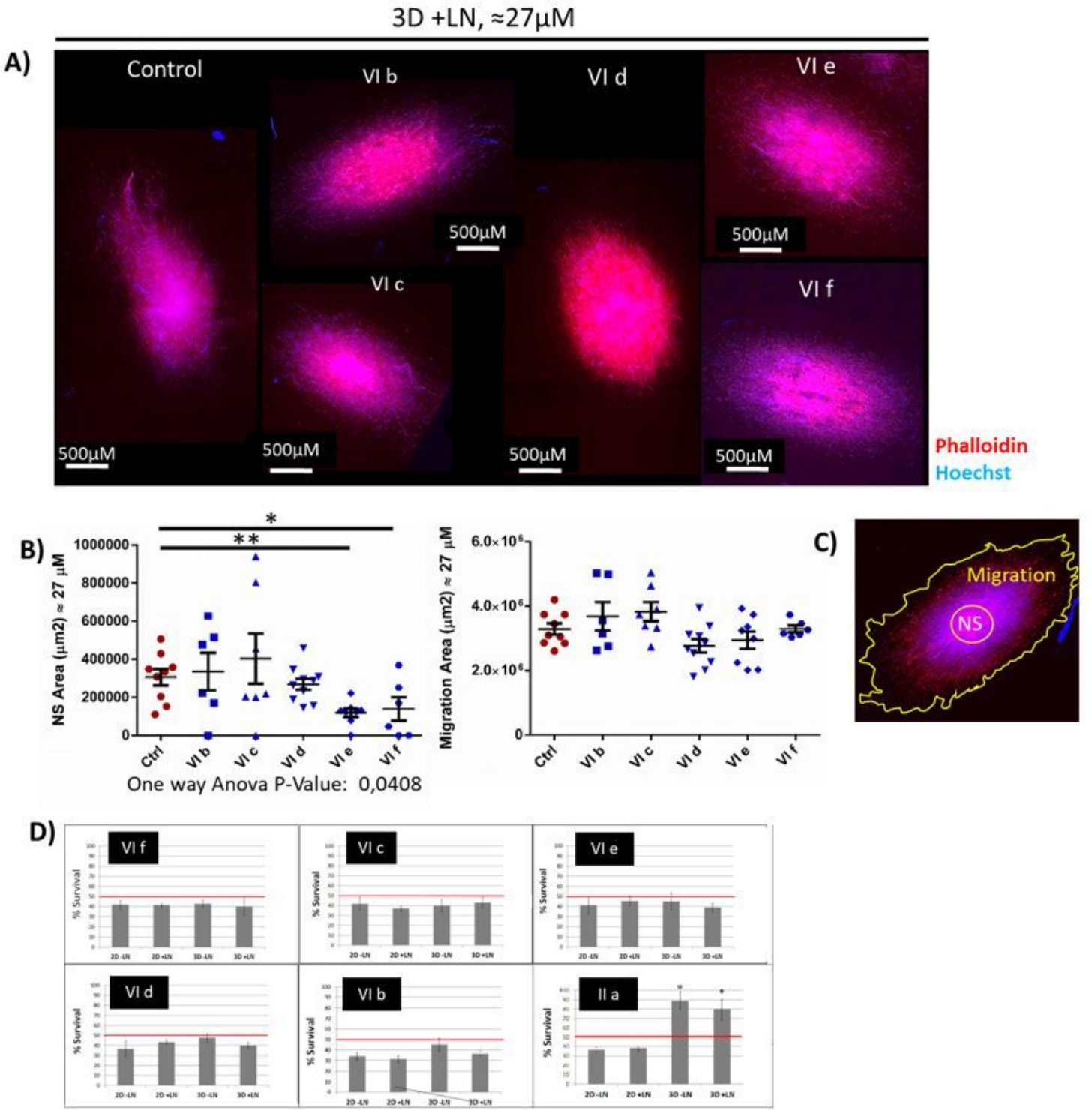

Figure 1

A) 5000 cells NS deposited on 3D +LN after 5 days of migration and percent survival of cell proliferation of the tested compounds obtained from the 2D and 3D GBM cell cultures with (2D+LN or 3D+LN) or without (2D-LN or 3D-LN) laminin. VIf, VIc, VIe, VId, VIb and IIa.

Supplementary Files

This is a list of supplementary files associated with this preprint. Click to download.

- scheme1.jpg
- scheme2.jpg
- scheme3.jpg
- scheme4.jpg
- scheme5.jpg
- scheme6.jpg
- scheme7.jpg